Journal of Molecular Structure, 159 (1987) 207—215
Elsevier Science Publishers B.V., Amsterdam — Printed in The Netherlands

SPECTROSCOPIC PROPERTIES OF THE Eu^{3+} ION IN THE $\{(C_4H_9)_4N\}_3Eu(NCS)_6$ CRYSTAL

W. STREK, E. MUGEŃSKI, R. CYWIŃSKI, J. HANUZA and
B. JEŻOWSKA-TRZEBIATOWSKA

Institute for Low Temperature and Structure Research, Polish Academy of Sciences, 50 950 Wroclaw (Poland)

H. MAGHRAWY

Chemistry Department, Nuclear Research Centre, Atomic Energy Commission, Cairo (Egypt)

(Received 12 September; in final form 31 October 1986)

ABSTRACT

The IR Raman and fluorescence spectra of Eu^{3+} in the $\{(C_4H_9)_4N\}_3Eu(NCS)_6$ crystal are reported. The results indicate that only one point symmetry of Eu^{3+} ion is present in the crystal. The presence of the $^5D_0 \rightarrow {}^7F_0$ transition in the fluorescence spectrum and the lack of strong vibronic lines indicates that the local symmetry of Eu^{3+} ion is lowered from O_h. The temperature dependence of fluorescence lifetimes of $^5D_0$ level has been measured. The mechanism of fluorescence quenching is briefly discussed.

INTRODUCTION

The spectroscopic properties of lanthanide(III) oxy compounds have been widely described. Much less work has been devoted to the non-oxygen bonded lanthanide(III) compounds. Recently, the six coordinated lanthanide(III) nitrogen coordination compounds were the subject of a few publications reporting their structural and spectroscopic properties [1—6]. The hexacoordinated complexes are very interesting for spectroscopic studies because of their tendency to form the highly symmetrical octahedral species. Such a symmetry was found for hexahalide $LnCl_6$ complexes [7]. A similar symmetry was found for pseudohalide complexes such as $(Et_4N)_3Yb(NCO)_6$ [8] and $(n\text{-}But_4N)_3Er(NCS)_6$ [1]. The spectroscopic properties of $(Et_4N)_3Eu(NCS)_6$ were reported by Bünzli and Klein [6] who found that the site symmetry of Eu^{3+} ion is not octahedral. A similar conclusion was reached by Malta et al. [4] who studied the mechanism of the $^5D_0 \rightarrow {}^7F_0$ transition of the Eu^{3+} ion in the $\{(C_4H_9)_4N\}_3Y(NCS)_6$ crystal.

In this paper we report the IR, Raman and luminescence spectra of $\{(C_4H_9)_4N\}_3Eu(NCS)_6$ crystal. The effect of temperature on quenching of the $^5D_0$ fluorescence is investigated.

0022-2860/87/$03.50

EXPERIMENTAL

Crystals of $\{(C_4H_9)_4\}_3Eu(NCS)_6$ were prepared by mixing both europium thiocyanate and tetra-n-butylammonium thiocyanate in a molar ratio of 3:1 respectively. They slowly crystallized from a 1:1 mixture of ethyl alcohol + t-butyl alcohol solution. The europium thiocyanate was freshly prepared stoichiometrically by mixing equivalent amounts of europium perchlorate and ammonium thiocyanate at room temperature. The corresponding europium perchlorate was prepared from europium oxide (POCh 99.9%) by dissolving in 10% perchloric acid solution. The tetra-n-butylammonium thiocyanate was prepared from the corresponding chloride salt (Ferak Berlin) treated by the equivalent weight of ammonium thiocyanate solution. The total analysis of the europium complex gave satisfactory agreement between the analytical calculation and that found. Satisfactory analyses for both Eu^{3+} and NCS^- have also been obtained.

Raman spectra were recorded with a JEOL S1 spectrophotometer. Spectra were excited with the 514.5 nm line of a Coherent Radiation argon ion laser. Spike filters were used to eliminate most of the plasma lines emitted by the laser. Light intensity focussed on the sample was approximately 300 mW.

IR spectra were measured in a Perkin Elmer 180 spectrophotometer using KBr and Nujol mull techniques.

The emission spectra were recorded in a conventional system. The excitation was performed with a high pressure xenon lamp XBO 150 and an SPM-2 (Zeiss Jena) monochromator. The emitted light was modulated by a chopper (400 Hz) and after passing the analyzing SPM-2 (Zeiss, Jena) monochromator was recorded by a system consisting of an M12FQS 51 photomultiplier, selective preamplifier (INTiBS), lock-in nanovoltmeter (type 232 UNIPAN) and a multichannel analyzer NTA-1024 (EMG) used as a ditital oscilloscope.

The fluorescence decay was measured in the same system using a low frequency chopper (2 Hz) in the excitation tract and a broad-band preamplifier (LM733) following the photomultiplier in the analyzing tract.

Additionally, systems of reference and triggering voltage as well as a programmable calculator (type 666 B EMG) cooperating with a multichannel analyser were used.

The measurements were performed in the temperature range 15—300 K using a microcooler Spectrim (CTI) and temperature controller (Oxford Instruments).

RESULTS

IR and Raman spectra

IR and Raman spectra of the $\{(C_4H_9)_4N\}_3Eu(NCS)_6$ crystal are shown in Fig. 1. These spectra were compared to those obtained for $\{(C_4H_9)_4N\}Cl$ as a reference sample to give a pure spectral pattern of the complex anion. The

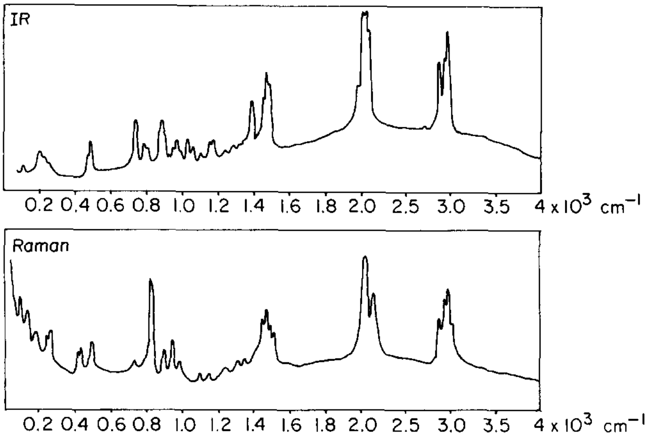

Fig. 1. The IR and Raman spectra of $\{(C_4H_9)_4N\}_3Eu(NCS)_6$ crystals.

wavenumbers, their relative intensities and some tentative assignments are shown in Table 1. According to crystallographic data [2, 3] in the $P\bar{1}$ (C_i) unit cell with $Z = 2$ each Eu^{3+} ion is bonded to six nitrogen atoms of thiocyanate ligand in an almost octahedral arrangement, although the symmetry is slightly distorted since the Ln—N—C angle is equal to 168—173°. The average Eu—N distance is 2.436 Å and all lanthanide—nitrogen bonds lie in the 2.422—2.462 Å range. The axial Eu—N bonds are clearly elongated in comparison to the equatorial-$Eu—N_4$ plane.

A factor group analysis based on the triclinic $P\bar{1}$ space group predicts 1068 unit-cell modes of which $3A_u$ are acoustic modes and 1065 optic modes. The optic modes can be further divided into external modes ($12A_g$ + $12A_u$ rotational and $12A_g$ + $9A_u$ translational) and internal modes of the cation ($459A_g$ + $459A_u$) and anion ($51A_g$ + $51A_u$). We observe only about 1/5 this number of bands and single crystal studies would be necessary to go further with this approach. The $Eu(NCS)_6^{3-}$ ion situated on the crystal site has C_1 symmetry when all atoms of the complex ion are considered. The local symmetry of the EuN_6 polyhedron seems to be higher than the symmetry of the lattice mode and may be considered as close to those of the tetragonal D_4 point group. This results from the following statement. After exclusion of the spectral pattern connected with vibrations of the cations, three types of bands remain: IR active modes, Raman active modes and both IR and Raman active ones. From the point group character tables it follows that such activity can only occur with D_4 symmetry.

The analysis of the IR and Raman spectra in the 50—4000 cm^{-1} range leads to the following conclusions:

(1) The ν(CN) vibrations appear in the IR spectrum as a complex multiplet built from the four main components at 2022—2084 cm^{-1} region. The shoulder at 1986 cm^{-1} appearing on the slope of the intense neighbour bands

TABLE 1

Wavenumbers, relative intensities and tentative assignment for the IR and Raman spectra of $\{(C_4H_9)_4N\}_3Eu(NCS)_6$ crystal

$(C_4H_9)N^+$ cation		$\{(C_4H_9)_4N\}_3Eu(NCS)_6$		Assignment
IR	Raman	IR	Raman	
2990 sh	2968 sh	2989 sh	2967 sh	$\nu(CH_3)$ of the cation
2958 s	2953 m	2958 s	2933 m	
2929 m	2914 m	2930 s	2913 m	
2870 m	2870 m	2869 s	2875 m	
		2084 sh	2079 s	$\nu(CN)$ of the complex anion
		2055 s		
		2037 vs	2037 vs	
		2022 vs		
		1986 sh		
1484 s	1497 m	1427 s	1495 m	$\delta_{as}(CH_3)$ of the cation
1467 s	1482 m	1472 s	1480 m	
1458 sh	1460 m	1462 s	1465 m	
1445 sh	1447 m	1450 sh	1452 m	
1396 sh		1380 m		$\delta_s(CH_3)$ of the cation
1382 m	1360 w	1360 w	1360 w	
	1288 w	1315 w	1290 w	Bending vibrations of the cation skeleton
		1280 w		
1245 w	1241 w	1241 w	1241 w	
1170 w	1153 w	1170 m	1153 w	
1150 m		1152 m		
1109 w	1108 w	1108 w	1109 w	
1065 w		1066 w		
1031 w		1055 w		
		1031 m		
	963 m	970 m	968 m	
		956 w		
925 w	908 m	926 w	908 m	
		894 sh		$\nu(CS)$ of the anion
		885 m	879 m	
		876 sh	814 vs	
794 m		799 m	744 w	$\rho(CH_3)$ of the cation
736 m		738 m		
		485 m	476 m	$\delta(MNCS)$ of the anion
		475 m	418 m	
			408 m	
		230 sh	258 s	$\nu(EuN)$ of the anion
		218 sh	248 s	
		202 m	196 m	
		113 vw	120 m	$\delta(NEuN)$ of the anion
			100 m	

are due to the $\nu(C^{15}N)$ or $\nu(^{13}CN)$ vibration. The Raman spectra in the region discussed exhibit a clear doublet at 2037 and 2079 cm^{-1}.

(2) The ν(CS) mode lies in the 810—890 cm^{-1} region which is consistent with the N-bonded thiocyanate coordination [9—11].

(3) Although the NCS group was found to be almost linear the degeneracy of the NCS bonding mode is resolved in the IR and Raman spectra. The IR splitting is small (10 cm^{-1}), but in Raman spectra the three components at 408, 418 and 476 cm^{-1} are observed.

(4) In the 190—260 cm^{-1} region the complex multiplet is observed belonging primarily to the ν(Eu—N) stretching vibration. In the Raman spectrum the three components are observed at 196, 248 and 258 cm^{-1}. The distinct splitting of the band observed in the region discussed is due to removal of the band degeneracy by the correlation effect in the unit cell and lowering of the symmetry from O_h to D_4 (and further to C_1).

(5) The bands at 113 cm^{-1} (IR) and 100—120 cm^{-1} (Raman) may be treated as δ(NEuN) bending vibrations. The anion spectrum is free from the bands in the FIR region.

Assuming the O_h nomenclature and the IR and Raman activities of the bands observed, the following energetic sequence of the vibrational modes may be proposed for the EuN_6 core: $\nu_1(A_{1g}) = 250$, $\nu_2(E_g) = 196$, $\nu_3(F_{1u}) = 202$, $\nu_4(F_{1u}) = 113$, $\nu_5(F_{2g}) = 110—120$ cm^{-1}.

The Urey—Bradley force constants evaluated for this set of wavenumbers are listed in Table 2. These dynamic parameters are close to those of other lanthanide complexes with nitrogen donor ligands [11].

Luminescence spectra

The luminescence spectrum of Eu^{3+} ions in $\{(C_4H_9)_4N\}_3Eu(NCS)_6$ was measured at 15 K and at room temperature. The low temperature spectrum is shown in Fig. 2. It consists of characteristic bands assigned to the $^5D_1 \rightarrow {}^7F_J$ and $^5D_0 \rightarrow {}^7F_J$ transitions. The assignments of the observed lines are listed in Table 3. The whole appearance of the spectra is analogous to that reported by Bünzli and Klein [6] for $(Et_4N)_3Eu(NCS)_6$. The $^5D_0 \rightarrow {}^7F_0$ transition is relatively weak but not split which indicates that only one Eu^{3+} site symmetry is represented in the crystal. This transition may occur only for C_s, C_n and C_{nv} point symmetries, so one can conclude that the Eu^{3+} symmetry is lowered from O_h. Also, the splitting of the ^7F_J levels into the Stark components indicates a lowering of the Eu^{3+} point symmetry from O_h.

Temperature dependence of decay times

The temperature dependence of fluorescence decay times of $^5D_0$ level is shown in Fig. 3. The observed decay curves were exponential. The decay time decreased significantly with increasing temperature from 3.5 ms at 15 K to 2.3 ms at 300 K. The high decay time at 15 K indicates that nonradiative

TABLE 2

Observed and calculated wavenumbers, Urey—Bradley force constants and potential energy distribution (PED 10%) for EuN_6 core of $\{(C_4H_9)_4N\}_3Eu(NCS)_6$

Mode	Wavenumbers			PED (%)[a]	Force constant (mdyn Å^{-1})
	Observed		Calculated		
	IR	Raman			
$\nu_1(A_1)$	—	258	247.6	$\Sigma\ 0.1627\ (r_1 + r_2 + r_3 + r_4 + r_5 + r_6)$	
$\nu_2(E_g)$	218	196	217.8	$0.159\ r_1 + 0.312\ r_3 + 0.312\ r_5 + 0.188\ r_6$	$K = 0.339$
	202		217.8	$0.172\ r_1 + 0.305\ r_2 + 0.305\ r_4 + 0.172\ r_6$	
$\nu_3(F_{1u})$	230	248	238.0	$\Sigma\ 0.1667\ (r_1 + r_2 + r_3 + r_4 + r_5 + r_6)$	$H = 0.084$
			229.3	$0.145\ r_1 + 0.318\ r_3 + 0.318\ r_5 + 0.145\ r_6$	
			229.3	$0.186\ r_1 + 0.298\ r_2 + 0.298\ r_4 + 0.186\ r_6$	
$\nu_4(F_{1u})$	113	120	124.1	$\Sigma\ 0.25\ (\alpha_1 + \alpha_2 + \alpha_3 + \alpha_4)$	$F = 0.032$
			124.1	$\Sigma\ 0.25\ (\alpha_5 + \alpha_7 + \alpha_9 + \alpha_{11})$	
			124.1	$\Sigma\ 0.25\ (\alpha_6 + \alpha_8 + \alpha_{10} + \alpha_{12})$	
$\nu_5(F_{2g})$	—	100	97.2	$\Sigma\ 0.231\ (\alpha_8 + \alpha_{10})$	
			97.2	$\Sigma\ 0.173\ (\alpha_1 + \alpha_3 + \alpha_5 + \alpha_{11})$	
			93.6	$\Sigma\ 0.144\ (\alpha_2 + \alpha_4 + \alpha_6 + \alpha_7 + \alpha_9 + \alpha_{12})$	
$\nu_6(F_{2u})$	—	—	87.8	$\Sigma\ 0.125\ (\alpha_5 + \alpha_6 + \alpha_7 + \alpha_8 + \alpha_9 + \alpha_{10} + \alpha_{11} + \alpha_{12})$	
			87.8	$\Sigma\ 0.125\ (\alpha_1 + \alpha_2 + \alpha_3 + \alpha_4 + \alpha_5 + \alpha_7 + \alpha_9 + \alpha_{11})$	
			87.8	$\Sigma\ 0.125\ (\alpha_1 + \alpha_3 + \alpha_3 + \alpha_4 + \alpha_6 + \alpha_8 + \alpha_{10} + \alpha_{12})$	

[a] Internal coordinate description: $r_i\ (i = 1$—$6)$; $\alpha_1(r_3, r_4)$, $\alpha_2(r_4, r_5)$, $\alpha_3(r_5, r_6)$, $\alpha_4(r_3, r_6)$, $\alpha_5(r_1, r_3)$, $\alpha_6(r_1, r_4)$, $\alpha_7(r_1, r_5)$, $\alpha_8(r_1, r_6)$, $\alpha_9(r_2, r_3)$, $\alpha_{10}(r_2, r_4)$, $\alpha_{11}(r_2, r_5)$, $\alpha_{12}(r_2, r_6)$.

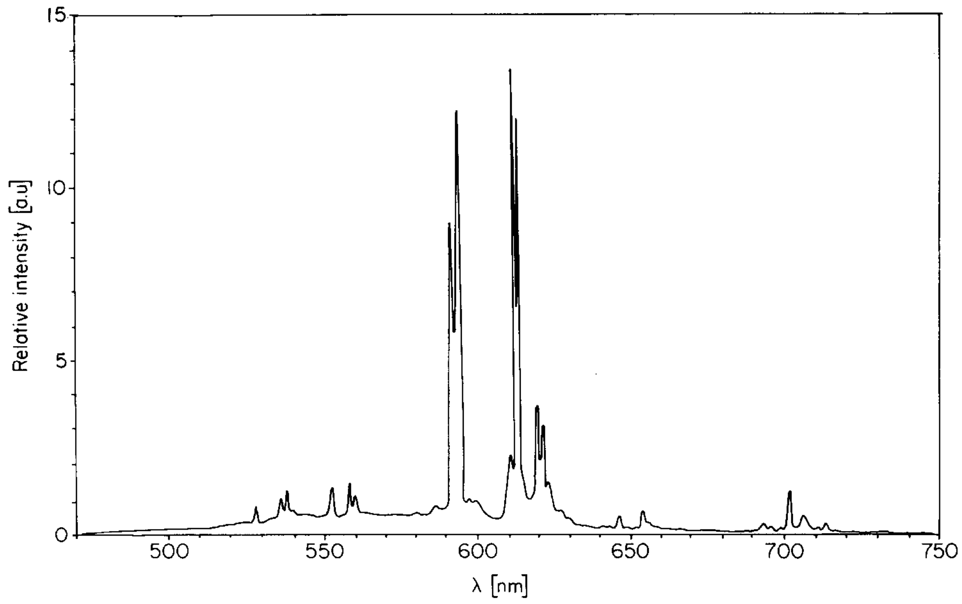

Fig. 2. The fluorescence spectra of $\{(C_4H_9)_4N\}_3Eu(NCS)_6$ crystals at 15 K.

relaxation processes play a minor role in deactivation of the $^5D_0$ level. This conclusion is supported by the large energy distance of $^5D_0$ from the lower lying $^7F_6$ level (energy gap rule [12]). At low temperature the rate constant of multiphonon relaxation is given by

$$W(T) = Be^{-\alpha\Delta E}(1 + \bar{n}_{\max})^{\Delta E/\hbar w_{\max}} \qquad (1)$$

where $\bar{n}_{\max}$ is the average occupation number of phonons of energy $\hbar w_{\max}$

$$\bar{n}_{\max} = [\exp(\hbar w_{\max}/kT) - 1]^{-1} \qquad (2)$$

The parameters B and α are characteristics of the crystal. Equation (1) constitutes a fact that the nonradiative relaxations in the lanthanide(III) system are controlled by the highest energy vibrations and the energy gap ΔE. These conclusions are well proved by experimental data.

To obtain an insight into the mechanism of temperature quenching of fluorescence decay times we have approximated the curve of temperature dependence in Fig. 3 by an Arrhenius exponent. In the range 70—250 K this curve is well fitted with an Arrhenius plot involving an activation energy E_A = 245 cm^{-1}. Since this energy is much lower than the maximum energy of phonons in our crystal (~3000 cm^{-1}) the temperature dependence of fluorescence is most probably associated with the energy migration enhanced by the thermal population of the lowest component of the $^7F_1$ level. In fact, the energy of the lower Stark component of this level (317 cm^{-1}, see Table 3) is close to the activation energy obtained from the Arrhenius plot.

TABLE 3

The energy of the observed transitions in the fluorescence spectrum of $\{(C_4H_9)_4N\}_3Eu(NCS)_6$ at 15 K

Transition	E (cm^{-1})	Transition	E (cm^{-1})
$^5D_1 \rightarrow {}^7F_0$	18949	$^5D_0 \rightarrow {}^7F_0$	17201
$^5D_1 \rightarrow {}^7F_1$	18630	$^5D_0 \rightarrow {}^7F_1$	16884
	18565		16839
$^5D_1 \rightarrow {}^7F_2$	18053		16817
	17876	$^5D_0 \rightarrow {}^7F_2$	16126
	17837		16109
$^5D_1 \rightarrow {}^7F_3$	17160		16080
	17128		16034
	17065		15982
	17030		15912
	16978		15870
		$^5D_0 \rightarrow {}^7F_4$	14441
			14423
			14386
			14284
			14197
			14177
			14105
			14086
			14055
			14034
		$^5D_0 \rightarrow {}^7F_5$	13705

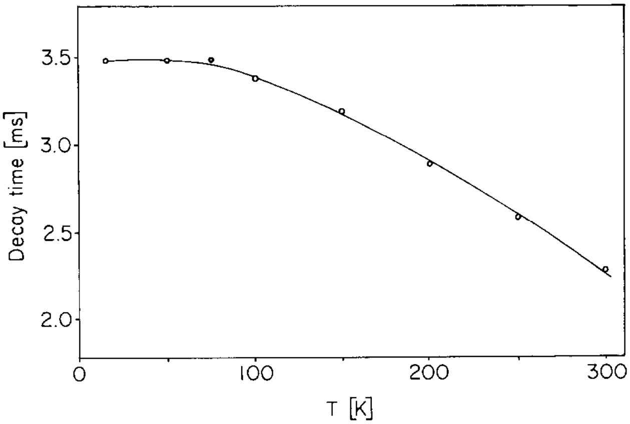

Fig. 3. The temperature dependence of fluorescence decay time of $^5D_0$ fluorescence of $\{(C_4H_9)_4N\}_3Eu(NCS)_6$.

CONCLUSIONS

In this paper, the IR, Raman and fluorescence spectra of Eu^{3+} in $\{(C_4H_9)_4N\}_3Eu(NCS)_6$ crystal are reported. The results indicate that the local symmetry of Eu^{3+} ion in this crystal is slightly lowered from O_h symmetry. This small distortion of the EuN_6 polyhedron affects the vibrational spectra less than the fluorescence spectra of the crystal. No strong phonon-assisted transitions were found in fluorescence. From the measurements of fluorescence decay times one can conclude that the multiphonon relaxation combined with the highest energy vibrations located at the counter ions do not contribute significantly to deexcitation of the $^5D_0$ level. The temperature dependence of fluorescence decay times is explained by the anti-Stokes diffusion between Eu^{3+} ions.

ACKNOWLEDGEMENT

One of the authors (H. Maghrawy) wishes to thank both the Ministry of High Education and the Polish Academy of Sciences for supporting the research cooperation.

REFERENCES

1 J. L. Martin, L. C. Thompson, I. J. Raclovich and M. D. Slick, J. Am. Chem. Soc., 90 (1968) 4493.
2 R. H. de Almeida Santos and J. R. Lechat, Quim. Nova, L. 63 (1980).
3 R. H. de Almeida Santos and J. R. Lechat, J. Solid. State Chem., 3 (1982) 87.
4 O. L. Malta, W. M. Azevedo, E. A. Gouiveia and G. F. De Sa, J. Lumin., 26 (1982) 337.
5 L. Hiltunen, J. Hölsä, W. Strek and B. Jeżowska-Trzebiatowska, J. Less-Common. Met., in press.
6 J.-C. G. Bünzli and B. Klein, Inst. Phys. Conf. Ser., 37 (1978) 115.
7 L. R. Morss, M. Siegal, L. Stenger and N. Edelstein, Inorg. Chem., 7 (1970) 1771.
8 H. D. Amberger, R. D. Fischer and G. G. Rosenbauer, Z. Naturforsch, Teil B, 31 (1976) 1.
9 J. Lewis, R. S. Nyholm and P. W. Smith, J. Chem. Soc., (1961) 4590.
10 A. Turco and C. Pecile, Nature (London), 191 (1961) 66.
11 R. A. Bailey, S. L. Kozak, T. W. Michelson and W. Mills, Coord. Chem. Rev., 6 (1970) 407.
12 R. Reisfeld and C. K. Jorgensen, Lasers and Excited States of Rare Earths, Springer Verlag, Berlin, 1977.